Available online at www.sciencedirect.com
SCIENCE DIRECT
Journal of Molecular Catalysis A: Chemical 252 (2006) 125–131
JOURNAL OF MOLECULAR CATALYSIS A: CHEMICAL
www.elsevier.com/locate/molcata

Acid site accessibility in sulfonated polystyrene acid catalysts: Calorimetric study of NH_3 adsorption from flowing gas stream

Prem Felix Siril, David R. Brown *

Department of Chemical and Biological Sciences, University of Huddersfield, Huddersfield, HD1 3DH, UK

Received 22 December 2005; received in revised form 14 February 2006; accepted 15 February 2006
Available online 27 March 2006

Abstract

Calorimetric pulsed NH_3 adsorption measurements from a flowing carrier gas have been made on sulfonated poly(styrene-*co*-divinylbenzene) resin acid catalysts to characterise surface acidity in general and acid site accessibility in particular. The adsorption and enthalpy profiles associated with each pulse of NH_3 show distinct features associated with relatively weak and reversible adsorption of NH_3 followed by strongly exothermic reaction with sulfonic acid sites and irreversible adsorption. The rate at which NH_3 diffuses from its initial adsorption site to an acid site is shown to depend on catalyst particle size, adsorption temperature and the proportion of unreacted acid sites. By varying the contact time of NH_3 with the catalyst the reversibility of the initial NH_3 adsorption is demonstrated and an increasing number of the acid sites within the polymer matrix are shown to become completely inaccessible to NH_3 as the contact time is reduced.

Keywords: Solid acid catalysts; Flow adsorption calorimetry; Ammonia; Sulfonated polystyrene; Amberlyst 15; Acid site accessibility; Adsorption kinetics

1. Introduction

Polystyrene supported sulfonic acid resins are widely used as acid catalysts in the production of ethers for the petrochemical industry [1–4], esterification [5–10], ester hydrolysis [11], alkene hydration [12–14] and other reactions [15–18]. They offer advantages over typical inorganic solid acids through their high concentrations and uniformity of acid sites, but disadvantages in that they are not stable above 150 °C and the strength of the acid sites are generally regarded as being relatively low (in part because complete dehydration of the sites is not possible). Another important factor in their use as catalysts is that they do not have a conventional surface and access to acid sites requires diffusion through the sulfonated polymer matrix. This is facilitated in water because the matrix hydrates and swells but in non-swelling solvents diffusion is restricted. Conventional sulfonated resins are prepared as uniform beads, often known as "gel" resins. Because of restricted diffusion, the majority of acid sites in these materials are only accessible when the beads are fully swollen. A second type, the so-called "macroporous" sulfonated resins, are also supplied in the form of small beads but are prepared with permanent porosity, and are designed to allow access to more of the acid sites even in non-swelling solvents. Even here, however, some diffusion through the matrix will always be necessary for reactant to reach acid sites.

Understanding the extent to which reaction rates in both gel and macroporous sulfonated resins are under internal diffusion control is not easy, since there will always be a distribution of active sites, from those close to the catalyst surface for which diffusion distances from the reaction medium are short, to those deep in the matrix for which significant diffusion is required. Reaction rates at some of the sites may be kinetically controlled whereas at others it may be diffusion controlled, and for the least accessible sites the contribution they make to the reaction rate may be negligible. Meaningful characterisation of the acid catalytic properties of these materials requires that the accessibility of acid sites, as well as their abundance and strength, be studied.

We have already published a number of studies of the acid strengths of various sulfonated polystyrene resins by NH_3 adsorption calorimetry, interpreting the amount of NH_3 adsorbed and the molar enthalpy of adsorption in terms of the abundance and strength of acid sites [13,14,19–21]. To make these measurements, a series of pulses of NH_3 were introduced

* Corresponding author. Tel.: +44 1484473397; fax: +44 1484472182.
E-mail addresses: spfelix@yahoo.com (P.F. Siril), d.r.brown@hud.ac.uk (D.R. Brown).

1381-1169/$ – see front matter © 2006 Elsevier B.V. All rights reserved.
doi:10.1016/j.molcata.2006.02.050

to the dried resins at 100 °C in an otherwise evacuated system. Each pulse of NH_3 was allowed to equilibrate with the resin catalyst. We found that, with macroporous resins, total NH_3 uptake was equivalent to stoichoiometric adsorption on all the acid sites on the resins and, once these were saturated, further adsorption was minimal and with very low associated enthalpies of adsorption. We concluded that NH_3 is capable of diffusion from the macropores in these beads into the matrix to reach all sulfonic acid groups, provided that sufficient time is given for equilibrium to be achieved. (Interestingly, similar experiments with gel resins, where there is no porosity, showed that only ca. 5–10% of acid sites were accessible to NH_3 under the same conditions [13].)

We have recently developed a modified calorimetric adsorption technique in which NH_3 is introduced in pulses to a flowing carrier gas and then passed over a sample in a flow-through calorimeter cell [19]. The crucial differentiating feature of this technique is that the contact time of the NH_3 with the catalyst can be controlled. This allows us to study the rate of reaction between NH_3 and acid sites and therefore the accessibility of acid sites. In the work reported here we have applied this flow calorimetric technique to the adsorption of NH_3 by both macroporous and gel-type sulfonated polystyrene resins, and we attempt to demonstrate the value of this technique in predicting catalytic properties.

2. Experimental

Two commercially available sulfonated poly(styrene-*co*-divinylbenzene) resins were used: macroporous Amberlyst 15 (Rohm and Haas) and gel type C100H (Purolite). Both were supplied in the acid form as beads. They were dried at 100 °C for 1 h before use. In both cases bead diameters varied from approximately 0.4–1.2 mm. Samples were fractioned into beads with diameters greater and less than 0.8 mm. In addition, beads were ground to powders (facilitated by cooling) and the $\leq$125 μm fraction collected.

A detailed description of the experimental set up for pulse flow calorimetry can be found in [19]. In a typical experiment, an accurately weighed sample is transferred to the DSC (Setaram DSC 111) sample tube and activated under a flow of helium at an elevated temperature. The activation temperature used here was generally 100 °C, except where adsorption experiments were to be performed at 150 °C in which case activation was also carried out at this higher temperature. A sequence of metered pulses of probe gas (1% NH_3 in He) is then injected to the carrier gas stream and passed through the sample. The DSC detects any heat changes as the probe interacts with the sample and the downstream thermal conductivity detector (TCD) is used to monitor NH_3 concentration in the gas after contact with the catalyst. Time (1.5 h) is allowed between each pulse to allow reversibly adsorbed NH_3 on the sample to desorb back into the carrier stream and/or redistribute on the sample, and for the baselines to stabilise. The net heat evolved during each pulse and the net amount of NH_3 adsorbed irreversibly can be calculated for each pulse (taking the difference between the peak area above and below the baselines for pulses where desorption follows adsorption). The differential molar enthalpy of adsorption, ΔH°_{ads}, associated with irreversibly adsorbed NH_3 from each pulse is plotted against the total amount of NH_3 irreversibly adsorbed per gram of the sample, or surface coverage. The dry mass of the sample is determined by weighing at the end of each experiment and is used for calculating the surface coverage after subtracting the mass of adsorbed NH_3. In the work reported here multiple experiments were performed on each sample keeping the conditions the same, and satisfactory reproducibility was achieved for both DSC and TCD peak integrations.

3. Results and discussions

Typical outputs are shown in Fig. 1 for NH_3 adsorption on Amberlyst 15 at 100 °C, with a 5 ml min^{-1} flow rate of the carrier gas into which 5 ml pulses of the NH_3/He mixture (2.065 μmol NH_3) were injected at regular intervals. The first channel is the TCD output and the second channel is the DSC thermal curve. The TCD and DSC responses during the activation of the catalyst before the adsorption experiment are not shown. The activation time was chosen to ensure that baselines in both channels were re-established after the broad endotherm and associated TCD signal resulting from sample water loss.

The peaks in the TCD output are due to NH_3 in the carrier gas downstream of the sample. The way in which the TCD data is presented needs some explanation. Firstly, the TCD output measured when a control pulse of NH_3 was passed through an empty sample tube was recorded. A typical peak for such a control pulse has been added to the figure to illustrate this. So that the amount of NH_3 adsorbed from each pulse during an experiment can be quickly gauged from the figure, the area of the control peak has been subtracted from every TCD peak measured during an adsorption experiment, and it is these "difference" peaks that are shown in Fig. 1. This means that a peak below the baseline corresponds to NH_3 adsorption by the sample, and comparison with the control pulse peak shows how much of the NH_3 pulse has been adsorbed from any one pulse. To clarify, a flat baseline would be generated by a pulse that passed through the sample bed without adsorption and a downward peak the same size as the control peak would indicate that the entire pulse had been adsorbed. Peaks seen above the baseline correspond to desorption of NH_3 from the sample into the gas flow.

The DSC output shown in Fig. 1 is the raw data, and shows exotherms associated with NH_3 adsorption. Note that the control pulse (no sample) produces a very small exothermic peak (just visible), presumably linked to the change in thermal conductivity of the gas stream through the DSC cell as NH_3 is added. A correction to all adsorption enthalpy measurements is made for this, but it is essentially negligible.

The TCD data in Fig. 1 shows that a decreasing fraction of each pulse of NH_3 was adsorbed by the Amberlyst 15 beads up to the fifth pulse. For the fifth pulse through to the end of the experiment the fraction of each NH_3 pulse adsorbed is fairly constant, but adsorption is followed by some desorption, the extent of which increases as the experiment progresses. The calorimetric data largely follows this pattern, with exothermic signals

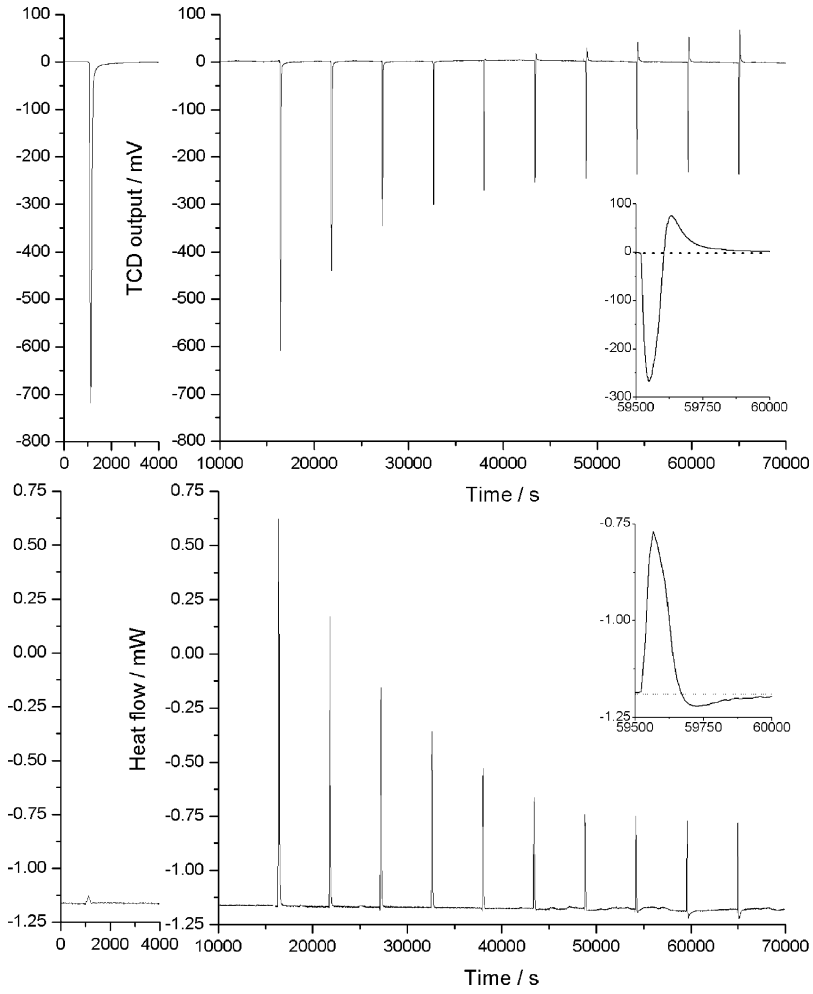

Fig. 1. Typical TCD and DSC output for NH_3 adsorption on 1.3 mg of Amberlyst 15 resin beads at 100 °C, 5 ml min^{-1} flow rate of He carrier gas and 5 ml pulses of 1% NH_3/He. The output for a 5 ml pulse of 1% NH_3/He through the blank sample tube is also shown. The ninth pulse is highlighted and shown in the inset. The effect of desorption of reversibly adsorbed NH_3 as the pulse passes is clearly visible.

associated with adsorption and endothermic signals associated with desorption.

From the data in Fig. 1 the molar enthalpy of NH_3 adsorption (ΔH°_{ads}) has been calculated for each pulse and plotted against the cumulative NH_3 adsorption or coverage (in mmol g^{-1}) in Fig. 2. The following points can be made about the data in Figs. 1 and 2. Strong adsorption occurs first on sites for which ΔH°_{ads} is around −115 kJ mol^{-1}. When these are saturated there is an abrupt fall in the amount of irreversible adsorption from each pulse and the associated ΔH°_{ads}. This occurs at a coverage of 4–5 mmol g^{-1}, which corresponds to the known total concentration of acid sites in the Amberlyst 15. So, assuming stoichiometric adsorption, it appears that all acid sites in Amberlyst 15, even when the resin is dry and unswollen, are accessible to NH_3 under these flow conditions. This mirrors the results of equivalent experiments where NH_3 adsorption was performed in a static system and was allowed to reach equilibrium after each pulse [13,14,19].

However, the data shown here differs from that measured under static conditions in that the fraction of each NH_3 pulse

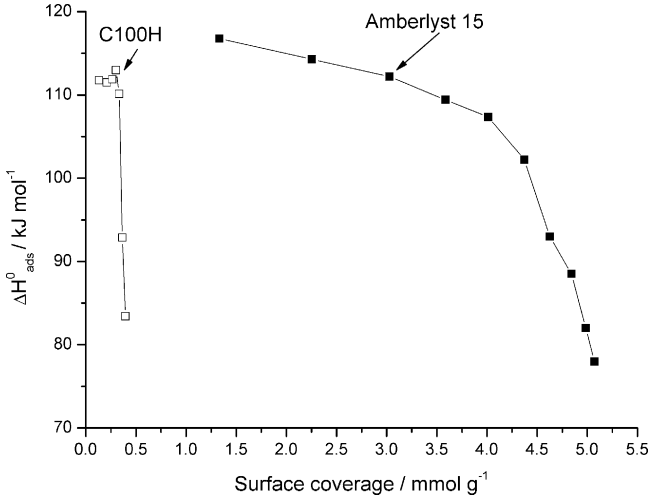

Fig. 2. Differential molar enthalpy of NH_3 adsorption (ΔH°_{ads}) vs. amount of NH_3 adsorbed (coverage) on beads of Amberlyst 15 (1.3 mg) and C100H (3.5 mg) at 100 °C, 5 ml min^{-1} flow of He and 5 ml probe gas injections.

adsorbed by the resin, or sticking factor, decreases quite markedly as the experiment proceeds (Fig. 1). In the static experiment, where time is allowed for equilibrium to be achieved after each addition of NH_3, the resin adsorbs virtually 100% of each pulse of NH_3 until all acid sites are saturated [13,14,19]. A further difference between data from the two techniques is in the way reversible adsorption, seen only for the later pulses, is immediately distinguishable from irreversible adsorption when using the flow technique.

A similar experiment was performed on the gel type C100H sulfonated resin beads. This material has no permanent porosity but has approximately the same concentration of acid sites as the macroporous Amberlyst 15. The ΔH°_{ads}/coverage profile is also shown in Fig. 2. In this case, very little NH_3 was irreversibly adsorbed, corresponding to less than 10% of acid sites. This result is broadly similar to that observed under equilibrium conditions in static experiments [13,14].

3.1. Effect of particle size

The effect of particle size on NH_3 adsorption from a flowing gas stream was examined using three size fractions of Amberlyst 15 (beads less and greater than 0.8 mm diameter and powder of particle size $\leq$125 μm). As would be expected, the sticking factors for NH_3 increased as the resin particle size was decreased. Further, the shapes of the DSC output for NH_3 adsorption on the three sizes of particle varied significantly. This can be seen in Fig. 3, which shows the outputs from experiments using the three fractions. The plots in Fig. 3 correspond to adsorption of the first, third and sixth NH_3 pulses. These are based on the same weights of the three fractions. The plot of ΔH°_{ads} versus surface coverage profile (not shown) were similar giving an average value of about $-115\,kJ\,mol^{-1}$ and final coverage of about $4.7\,mmol\,g^{-1}$ for all the three particle sizes.

From Fig. 3 it can be seen that the DSC outputs for the first pulse for the three fractions are very similar to each other. The outputs for the third pulse differ in shape from those of the first in that they are slightly broader and the peak maximum is delayed. In fact two peaks can be seen clearly for the larger beads. The signals recorded for the sixth peaks are different again, with the powder and the smaller beads giving narrower peaks and the larger beads still showing two peaks. Notice that for the powder an endothermic desorption process can also be seen.

A possible explanation for these peak shapes might be that there are two distinct processes occurring as NH_3 is adsorbed on the resins and that the enthalpy profiles are, in some cases, the superimpositions of two peaks. For the first pulse of NH_3, the DSC signals shown in Fig. 3 suggest that the two processes occur relatively close together. In the third pulse, which is roughly half way through the reaction between NH_3 and the acid sites, the two processes are well separated, increasingly so going from powder to small beads and to large beads. In the sixth pulse, where for the powder virtually all acid sites have reacted, a single exothermic process appears to occur, and the DSC signal is now much narrower than for the earlier pulses. For the beads, especially the larger beads, the dual exothermic processes can still be seen.

It seems that initial adsorption from the flowing gas by the resin occurs relatively quickly. The NH_3 then diffuses through the polymer matrix to unreacted acid sites, reaction at which gives rise to the second peak. The diffusion time increases as acid sites are progressively neutralised and the distance over which

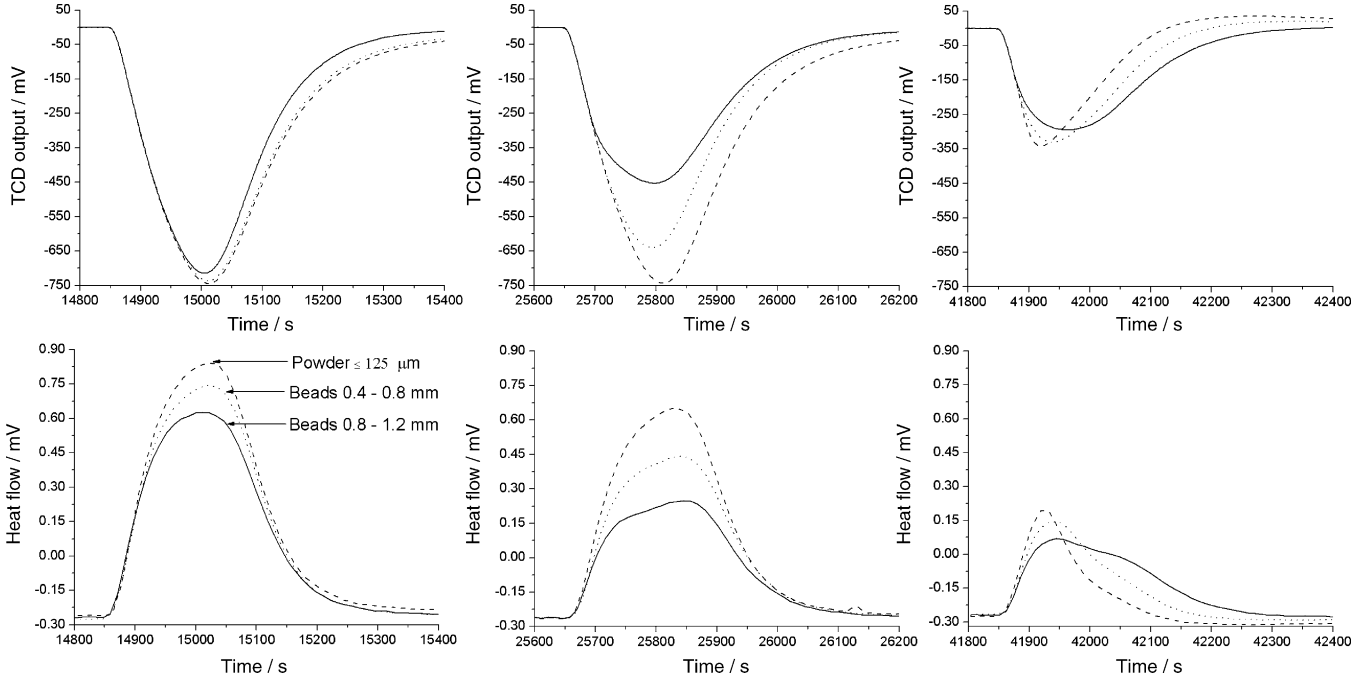

Fig. 3. Typical TCD and DSC outputs corresponding to adsorption from the first, third and sixth pulses of NH_3/He on samples of Amberlyst 15 (~1.5 mg) of varying particle size (beads 0.8–1.2 mm, beads 0.4–0.8 mm and powder $\leq$125 μm) at 100 °C, 2 ml min^{-1} flow rate and with 5 ml probe gas injections.

adsorbed NH_3 has to diffuse to reach an acid site increases. Once all acid sites are reacted (as for pulse six for the powder sample) all NH_3 adsorbed during initial contact remains only weakly held; there is no transition to chemisorption and once the NH_3 pulse is past almost quantitative desorption of the NH_3 occurs. This shows up as a narrow exothermic peak for initial adsorption followed by a broad endothermic feature as a large part of the adsorbed NH_3 desorbs.

A similar phenomenon where heat output peaks get broader as chemisorption progresses and then become narrow when only physisorption is occurring has been observed with oxygen on activated carbon [22]. Interestingly these authors saw this effect in a static system in which successive pulses of oxygen were allowed to reach equilibrium with the activated carbon adsorbent.

To investigate these processes further, the TCD and DSC output for the first pulse of NH_3 passing over the larger Amberlyst 15 beads has been analysed in detail. This is shown in Fig. 4. Note that in this figure the DSC and TCD outputs are plotted on the same time scale. From the peak onset times in the two plots it is clear that the time taken for gas to flow from the calorimeter cell to the TCD is only a few seconds. This means that any time differences between adsorption events (TCD) and thermal events (DSC) in the two plots are not due to any delays in NH_3 reaching the TCD but reflect the relative rates at which adsorption and thermal events occur on the sample.

From Fig. 4 it can be seen that the maximum heat output occurs around 20 s after the maximum in the adsorption profile, and the heat peak is very much broader showing significant levels of heat in the tail at times when adsorption is minimal. To confirm this, the apparent ΔH°_{ads} has been calculated for individual 15 s slices taken through both plots, and these are plotted together with the amount adsorbed during each of these slices. Note that the apparent ΔH°_{ads} calculated over each slice is numerically lower through the first 75–90 s than the average ΔH°_{ads} for this pulse of $-119\,kJ\,mol^{-1}$. After this time, the apparent ΔH°_{ads} climbs rapidly to very high values. This is consistent with the model described above. The initial low values of ΔH°_{ads} correspond to the indiscriminate adsorption of NH_3 by the resin. As this NH_3 diffuses and reacts with acid sites, the larger heats evolved then combine with the initial heats from more NH_3 adsorbing on the resin, giving rise to the delayed maximum in the heat output. Towards the end of the adsorption process, the continuing heat evolution is linked to previously adsorbed NH_3 finding acid sites and reacting.

The results of experiments with the gel resin C100H further illustrate the importance of diffusion distances in controlling effective acidity. This material has no permanent porosity and, in bead form, the majority of acid sites in the resin are completely inaccessible to NH_3, as described above. However, we also carried out flow calorimetric experiments on this resin in powdered form (particle size $\leq 125\,\mu m$). In marked contrast to the results with beads, we found that NH_3 adsorption on the powder proceeded in essentially the same way as on the macroporous Amberlyst 15 powder, with similar sticking factors and peak widths throughout the adsorption. We obtained similar ΔH°_{ads} versus surface coverage plots for the two powders, indicating

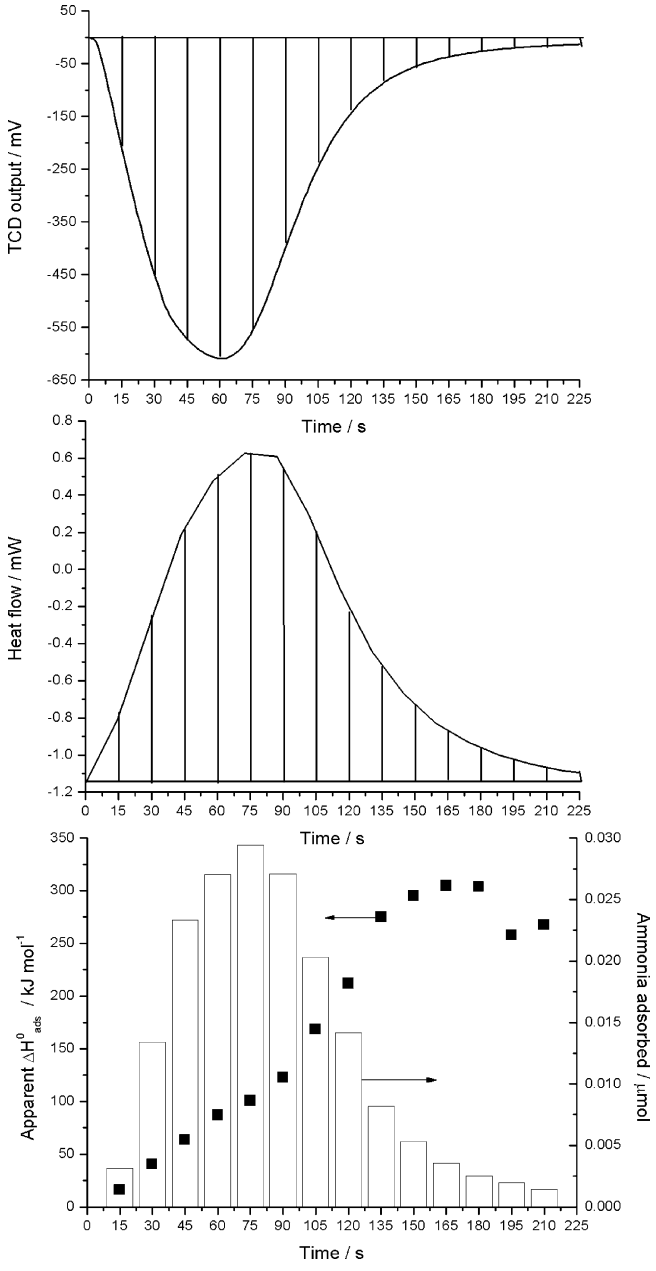

Fig. 4. TCD and DSC output for adsorption from the first 5 ml pulse of NH_3/He compared over 15 s intervals on Amberlyst 15 beads at 100 °C and 5 ml min^{-1} flow rate.

similar strengths of acid sites on both. These results suggest that, when ground to a fine powder, accessibility of acid sites is associated with the exposed external surface of the resin and is not related to the presence or absence of the porosity built into the original beads.

3.2. Effect of flow rate

The flow rate of carrier and the pulses of He/NH_3 dictate the contact time between NH_3 and the catalyst. We performed NH_3 adsorption experiments on Amberlyst 15 resin beads (as supplied) at 5, 10 and 15 ml min^{-1} flow rates. The ΔH°_{ads} versus coverage profiles are shown in Fig. 5. Except for the different

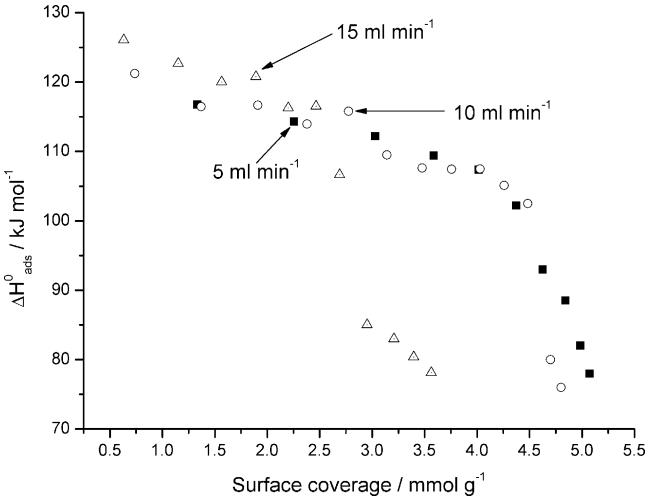

Fig. 5. Dependence of (ΔH°_{ads}) vs. NH_3 coverage profile for Amberlyst 15 resin beads on flow rate of He and He/NH_3 when 5 ml pulses of 1% NH_3/He were injected at 100 °C.

flow rates, the three experiments were identical. Comparing the data at 5 and 10 ml min^{-1} it can be seen that almost twice as many pulses were needed to saturate the resin at the higher flow rate. In other words, increasing the flow rate from 5 to 10 ml min^{-1} roughly halved the sticking factor for each pulse. However, the eventual concentration of NH_3 adsorbed by the resins on saturation was the same at the two flow rates.

Increasing the flow rate to 15 ml min^{-1} almost halved the sticking factor again (halving the amount of NH_3 adsorbed per pulse). Further, at this flow rate it became impossible to populate some of the acid sites – strong adsorption ceased beyond a cumulative adsorption of 2.5–3.0 mmol g^{-1}. Any adsorption beyond this amount was with a very low sticking factor and ΔH°_{ads} of numerically less than −85 kJ mol^{-1}. When this experiment was repeated with the powdered resin, even at 15 ml min^{-1} the profile was almost identical to that seen for the beads at 5 ml min^{-1} (in terms of both eventual adsorbed amount on strongly binding sites and sticking factors throughout).

Again, this is all consistent with a model in which weak NH_3 adsorption (largely reversible) by the beads is followed by a period in which the NH_3, remaining only weakly bound, diffuses through the matrix until acid sites are encountered, when strong binding ensues. The diffusion time depends on the particle size and the number of unreacted acid sites. After the NH_3 pulse passes, desorption of NH_3 that is still in weakly bound sites and has not yet reacted with acid sites is possible, and this accounts for the reduction in sticking factor seen as the NH_3 contact time is reduced.

3.3. Effect of adsorption temperature

Adsorption experiments were performed at 50, 100 and 150 °C on Amberlyst 15 beads as supplied. These experiments were carried out at the relatively low flow rate of 2 ml min^{-1}. This flow rate was used because the long NH_3/resin contact time prevents rapid desorption of weakly held NH_3. The TCD and DSC outputs for the first, third and sixth pulses are shown in Fig. 6. The adsorption/time profiles taken from the TCD outputs are virtually identical at all three temperatures for the initial pulse but for the subsequent pulses the 100 and 50 °C adsorption peaks become larger and broader than those at 150 °C. The heat

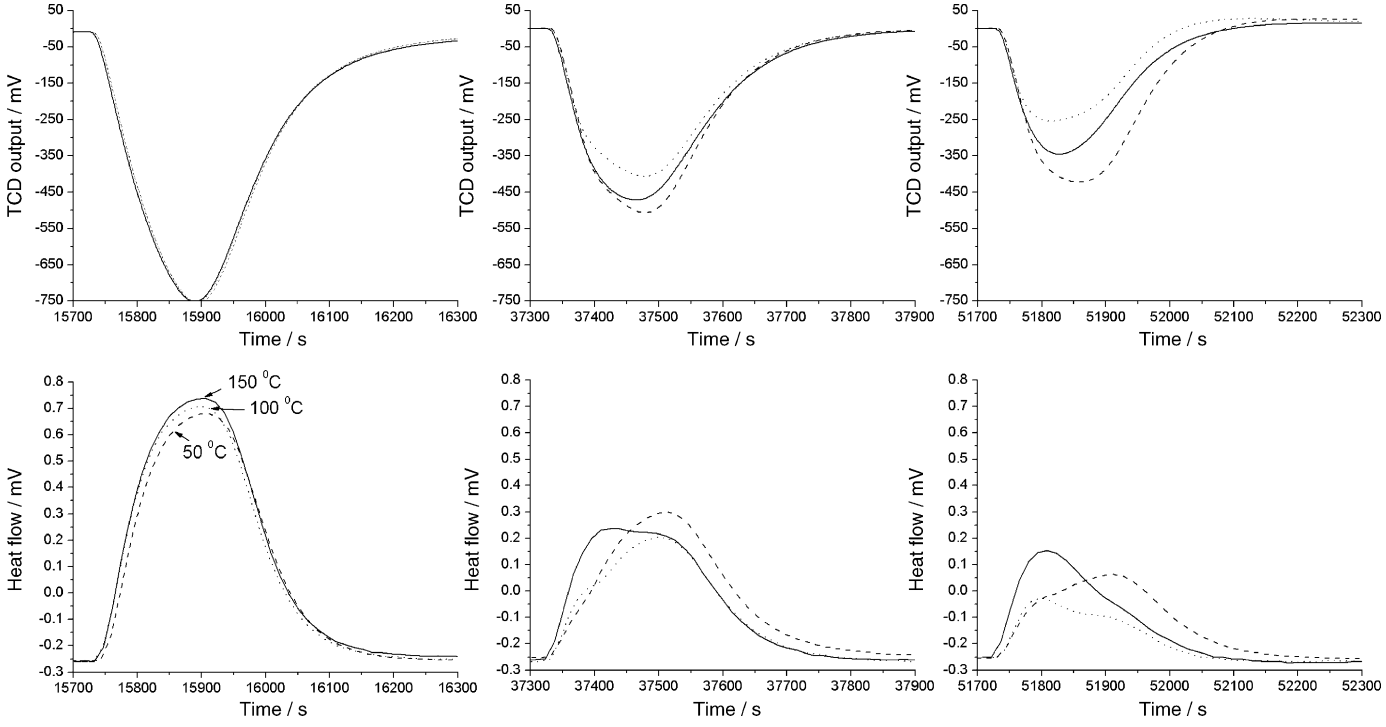

Fig. 6. Typical TCD and DSC outputs corresponding to the first, third and sixth pulses of NH_3 on Amberlyst 15 (~1.5 mg) at 50, 100 and 150 °C, at a flow rate of 2 ml min^{-1} with 5 ml probe gas pulses.

outputs are also similar at the three temperatures for the first pulse, but as adsorption progresses the heat output at the lower temperatures is increasingly delayed. This is most clearly seen by comparing outputs at the three temperatures for the sixth pulse adsorption. At 150 °C the heat and adsorption maxima almost coincide and the only feature of note on there are extensive tails in both adsorption and heat output. For the sixth pulse at 100 °C the adsorption peak is of similar shape to that at 150 °C but somewhat larger. The heat output at 100 °C shows a maximum at about the same time as the adsorption maximum but a distinct second peak about 100 s later. At 50 °C, the adsorption peak is broader and larger but the heat output is now very different, showing a relatively small first peak coincident with the adsorption maximum with a larger second peak following.

It is worth noting that the results for all earlier experiments were obtained at an adsorption temperature of 100 °C. The data in Fig. 6 shows that the adsorption process is very sensitive to temperature. Nevertheless, these results remain consistent with the weak adsorption/diffusion/strong adsorption model. At 150 °C the delayed heat output associated with NH_3 that has diffused through the matrix to acid sites is generally smaller than at 100 and 50 °C. This is almost certainly because, where significant diffusion to acid sites is required, the higher temperature both accelerates the diffusion process itself and also facilitates desorption of weakly bound NH_3 when the gaseous NH_3 above the sample is removed.

4. Conclusion

We have shown that the reaction between NH_3 and polystyrene supported sulfonic acid resins can be used as a probe for the accessibilities (as well as the abundance and strengths) of sulfonic acid sites. It appears that NH_3 is adsorbed relatively rapidly by all the sulfonic acid resins tested from a flowing gas stream. However, subsequent diffusion through the polymer matrix to a sulfonic acid site can take tens or even hundreds of seconds and, until the NH_3 reacts with an acid site, desorption of the NH_3 can occur back into the carrier gas stream. We have shown how the time taken for this internal diffusion step depends on the type of resin (macroporous or gel), the temperature and the extent to which the acid resin is already neutralised.

It may be argued that, in the case of sulfonated resin catalysts, the acid site accessibility in solvated swollen resins beads is of more relevance than accessibilities in dry resins [23]. This is undoubtedly true, but it is quite likely that diffusion rates of NH_3 and other simple probe molecules (especially potential hydrophobic reactants such as small alkenes) in dry resins is likely to reflect their relative behaviours in the swollen state. Given the simplicity of the flow calorimetric experiment, we believe that we have demonstrated the potential value of using this flow technique in the overall characterisation of solid acid catalysts.

Acknowledgement

Financial support from University of Huddersfield is gratefully acknowledged.

References

[1] A. Renhfiger, U. Hoffman, Chem. Eng. Sci. 45 (6) (1990) 1619.
[2] M. Iborra, J.F. Izquierdo, F. Cunill, J. Tajero, Ind. Eng. Chem. Res. 31 (1992) 1840.
[3] N. Boz, T. Dogu, K. Murtezaoglu, G. Dogu, Appl. Catal. A 268 (2004) 175.
[4] P.K. Pakkonen, O.I. Krause, React. Funt. Polym. 55 (2003) 139.
[5] Z.P. Xu, K.T. Chuang, Chem. Eng. Sci. 52 (17) (1997) 3011.
[6] W.T. Liu, C.S. Tan, Ind. Eng. Chem. Res. 40 (2001) 3281.
[7] M.T. Sanz, R. Murga, S. Beltran, J.T. Cabezars, J. Coca, Ind. Eng. Chem. Res. 43 (2004) 2049.
[8] M.T. Sanz, R. Murga, S. Beltran, J.T. Cabezars, Ind. Eng. Chem. Res. 41 (2002) 512.
[9] K. Jerabek, Z. Prakop, A. Revillon, React. Funct. Polym. 33 (1997) 103.
[10] S. Steinigweg, J. Gmehlong, Ind. Eng. Chem. Res. 41 (2002) 5483.
[11] C.M. Zhang, A.A. Adesina, M.S. Wainwright, Chem. Eng. Proc. Res. 42 (2003) 985.
[12] S.K. Ihm, M.J. Chung, K.Y. Park, Ind. Eng. Chem. Res. 27 (1988) 41.
[13] M. Hart, G. Fuller, D.R. Brown, C. Park, M.A. Keane, J.A. Dale, C.M. Fougret, R.W. Cockman, Catal. Lett. 72 (3/4) (2001) 135.
[14] M. Hart, G. Fuller, D.R. Brown, J.A. Dale, S. Plant, J. Mol. Catal. 182/183A (2002) 439.
[15] G.D. Yadav, R.D. Bhagat, J. Mol. Catal. 235A (2005) 98.
[16] J.S. Yadav, B.V.S. Reddy, B. Eshwaraiah, K. Anirudha, Green Chem. 4 (2003) 557.
[17] C. Ramesh, J. Banerjee, R. Pal, B. Das, Adv. Synth. Catal. 345 (2003) 557.
[18] P. Gogoi, Synlett 14 (2005) 2263.
[19] S.P. Felix, C. Savill-Jowitt, D.R. Brown, Thermochim. Acta 433 (2005) 59.
[20] D.R. Brown, C.N. Rhodes, Thermochim. Acta 294 (1997) 33.
[21] C.N. Rhodes, D.R. Brown, S. Plant, J.A. Dale, React. Funct. Polym. 40 (1999) 187.
[22] M. O'Neil, J. Philips, J. Phys. Chem. 91 (1987) 2867.
[23] B. Corain, M. Zecca, K. Jerabek, J. Mol. Catal. 177A (2001) 3.